Int. J. Microgravity Sci. Appl. **33**(1) (2016) 330107
DOI: 10.15011/jasma.33.330107

||||| Development of Boiling and Two-phase Flow Experiments on Board ISS |||||
(Original Paper)

Development of Boiling and Two-phase Flow Experiments on Board ISS
(Temperature Data Derivation and Image Analysis of a Transparent Heated Short Tube in the Glass Heated Section)

Masaki OKUBO [1], Osamu KAWANAMI [1], Kotaro NAKAMOTO [1], Hitoshi ASANO [2], Haruhiko OHTA [3], Yasuhisa SHINMOTO [3], Koichi SUZUKI [4], Ryoji IMAI [5], Satoshi MATSUMOTO [6], Takashi KURIMOTO [6], Michito SAKAMOTO [6], Hidemitsu TAKAOKA [6], Kenichiro SAWADA [6], Atsushi OKAMOTO [6], Haruo KAWASAKI [6], Masahiro TAKAYANAGI [6] and Kiyosumi FUJII [7]

Abstract

In order to clarify flow behavior and heat transfer characteristics of flow boiling in microgravity, the boiling and two-phase flow experimental facility which will be conducted in International Space Station (ISS) is developed. The glass heated section as an evaporating test section is installed in this facility, and the heated section is consisted of three transparent heated tubes which have different heated length, 50 mm, 50 mm and 5 mm, respectively. The transparent heated tube is made by Pyrex glass and the inner wall of the tube is covered by extremely thin gold film as using not only a heater but also resistance thermometer; that is, the tube can be measured the averaged inner wall temperature of the entire heated area. In addition, gas-liquid behavior of flow boiling can be observed through the gold film. The transparent heated short tube, which has 5 mm heated length and 4 mm inner diameter is a newly developed for third segment of the heated section of ISS experiment. In this study, derivation of the inner wall temperature and image analysis of flow behavior by using the short tube is described. Then the relation between heat transfer characteristics and flow behavior by using this tube is discussed. As a result of single-phase heat transfer experiment, the electrode resistance of the heated tube should be considerd for estimation of the inner wall temperature of the short tube. Nusselt number considered the resistance of the electrode part has a good agreement with existing correlations compeared to Nusselt number derived from total resistance of the tube. By using the image analysis, useful imformation such as liquid film thickness of annular flow and passing of disturbance wave can be obtained with heat transfer characteristics data simultaneously. The results indicates that the heat transfer in the liquid film region of slug flow is insignificantly small compeared to turbulent liquid flow at the wake of slug under the conditions of this study.

Keyword(s): Flow boiling, Flow behavior, Heat transfer, Image analysis
Received 1 January 2016; Accepted 25 January 2016; Published 31 January 2016

1. Introduction

For space applications in recent year, amount of exhaust heat, transporting distance of heat and heat generation density are increasing. In order to manage those thermal problems, flow boiling and two-phase system is a one of the effective way for the cooling system. To realize this system, thermal characteristics and flow behavior under microgravity conditions should be clarified, so flow boiling and two-phase flow experiment will be conducted in Japanese experimental module of International Space Station (ISS) at 2016 [1)]. In the experiment, two heated test section is installed; a glass heated section and a metal heated section. The metal heated section is a conventional one, it is made by copper tube with sheath wired heater. The glass heated section is included three transparent heated tubes in series. The transparent heated tube is developed by authors [2–4)], and it is made by Pyrex glass coated by transparent gold thin film on the inner wall of the tube. Simultaneous measurement of averaged inner wall temperature in the entire heated surface, heating of fluid, observation of flow behavior are possible by using this tube.

The three heated tubes in the glass heated section have a same inner diameter, 4 mm, but those have different the heated length. The heated length of two transparent heated tubes on the upstream side is 50 mm, and third heated tube located at the downstream has 5 mm of the heated length. So the third tube is called a transparent heated “short” tube, it is newly developed for ISS experiment. The short tube can observe flow behavior in detail, because ratio of its heated length to inner diameter (L/D) is very small and a camera which is used for observation of flow behavior can be located close to the short tube. The tube is used as a resistance

1 Dept. Mechanical Eng., University of Hyogo, 2167 Shosha, Himeji 671-2280, Japan.
2 Dept. Mechanical Eng., Kobe University, 1-1 Rokkodai, Nada-ku, Kobe 671-2280, Japan.
3 Dept.Aeronautics and Astronautics, Kyushu University, 744 Motooka, Nishi-ku, Fukuoka 819-0395, Japan.
4 Dept. Mechanical Eng., Tokyo University of Science, Yamaguchi, 1-1-1 Daigakudori, Sanyoonoda 756-0884, Japan.
5 Dept. Mechanical, Aerospace, and Materials Eng., Muroran Institute of Technology, 27-1 Mizumotocho, Muroran 050-0071, Japan.
6 Japan Aerospace Exploration Agency, 2-1-1 Sengen, Tsukuba 305-8505, Japan.
7 Nara Institute of Science and Technology, 8916-5 Takayama-cho, Ikoma 630-0192, Japan.
(E-mail: kawanami@eng.u-hyogo.ac.jp)

 © 2016 The Jpn. Soc. Microgravity Appl.
http://www.jasma.info/journal/

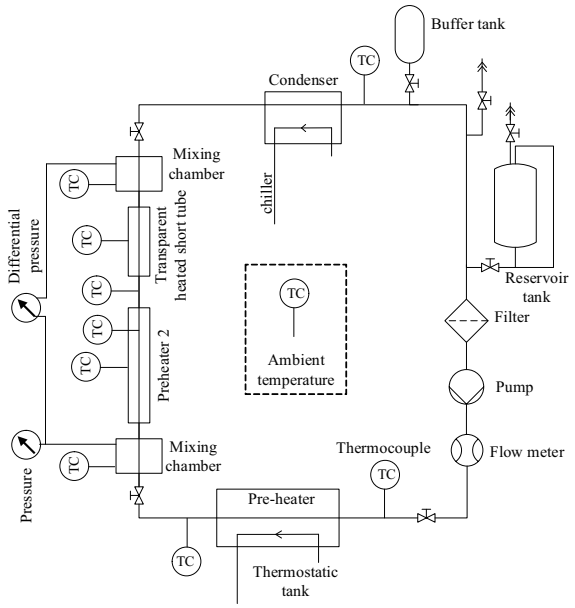

Fig. 1 Experimental setup.

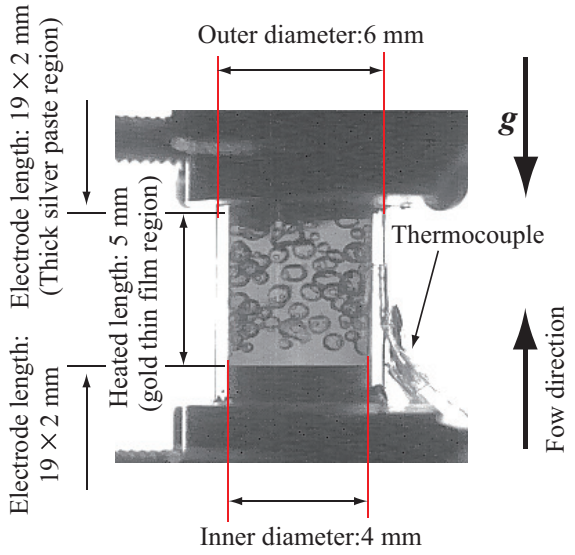

Fig. 2 Detailed structure of the heated section including a transparent heated short tube.

thermometer to estimate a inner wall temperature. However, the heated length of short tube is shorter than that of electrode part length, a resistance of electrode part should be considered to estimate the inner wall temperature.

In this paper, derivation of the inner wall temperature and image analysis of flow behavior by using the short tube under terrestrial conditions is described. Then, the relation between heat transfer characteristics and flow behavior is reported.

2. Experimental Setup and Data Analysis

2.1 Experimental Apparatus and Procedure

The experimental apparatus is shown in **Fig. 1**. The apparatus is consisted of a reservoir tank, pump, flow meter, preheater, metal heated tube, transparent heated tube, condenser, buffer tank. The metal heated tube is used as a second preheater, Preheater 2. Well-degassed FC-72 is used as a test fluid.

In this study, a transparent heated short tube as shown in **Fig. 2** is used as a heated section. The structure of the present short tube is a completely same as a heated tube of ISS experiment. The short tube has a 4 mm of inner diameter, 6 mm of outer diameter, 5 mm of the heated length. The transparent heated short tube is made by Pyrex glass and the inner wall of the tube is covered by extremely thin gold film as using not only a heater but also resistance thermometer; that is, the tube can be measured the averaged inner wall temperature of the entire heated area. In addition, gas-liquid behavior of flow boiling can be observed through the gold film. Detailed instruction about the transparent heated tube was reported in previous papers [2–4].

At the beginning of experimental run, the test fluid is well deaerated by a vacuum pump. The fluid is transfer from the reservoir tank to the heated section via two pre-heater sections by the pump. At the two pre-heater sections, the fluid is set at the desired conditions such as the subcooled temperature or quality at the inlet of a heated section. The fluid was heated and boiling occurred in the heated tube. The flow behavior and the thermal characteristics such as inner wall temperature should be measured simultaneously. Then the fluid is again became liquid single-phase by condenser part. The loop pressure at the inlet of the heated tube can be kept at a desired value by buffer tank.

The experimental conditions are listed in **Table 1**. Mass velocity, G , is 39 - 601 kg/m^2s, loop pressure at the inlet of the heated section, P_{in}, is around 0.1 MPa, heat flux, q_{in}, is 0 - 79 kW/m^2, and flow direction is vertical upward. Subcooling temperature or quality at the inlet of the heated section, ΔT_{sub} or x_{in}, are 0 - 42.8 K or 0 - 0.70, respectively.

Table 1 Experimental conditions.

Parameter	Range	Units
Test fluid	Degassed FC-72	-
Flow direction	vertical upward	-
Mass velocity G	39 - 601	kg/m^{2}s
Inlet pressure P_{in}	94.6 - 107.9	MPa
Inlet subcooled ΔT_{sub} / Inlet quality x_{in}	0 - 42.8 / 0 - 0.7	K / -
Heat flux q_{in}	0 - 79.0	kW/m^2

2.2 Temperature Data Derivation

As shown in **Fig. 2**, the heated tube has two electrodes located at the both end of the tube and a short heated part. The electrode region is covered by silver paste on the inner and outer wall of the tube. The thickness of the silver paste is 10-50 μm, it is quite thick compared to the gold film thickness which is 10-50

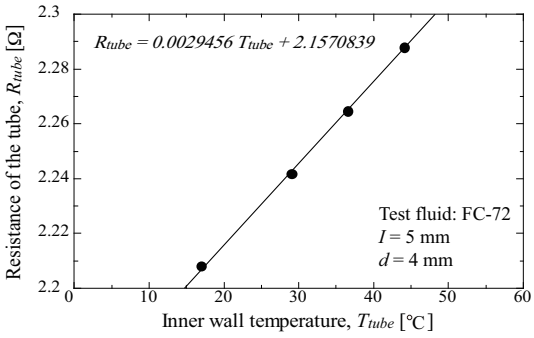

Fig. 3 The relation between the inner wall temperature T_{tube} and the resistance of the tube R_{tube}.

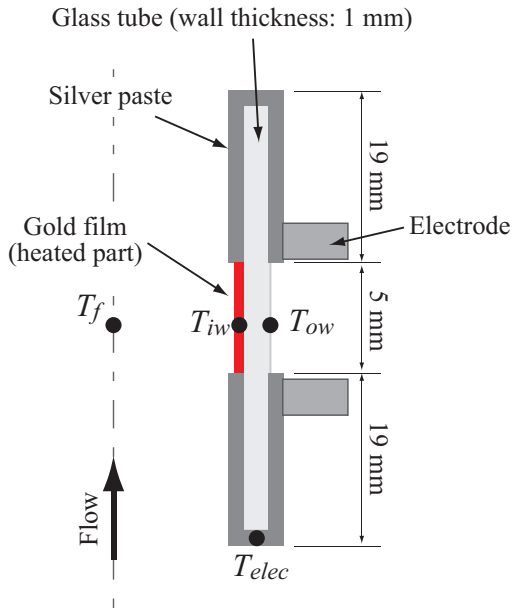

Fig. 4 The electro-structure of the transparent heated short tube (not to scale).

nm. Until now, the resistance of electrodes region was ignored as reported in previous papers[2–4], because the resistance of the heated part is substantially high compared to the resistance of the electrode region. In this case, the inner wall temperature can be estimated as a function of the tube resistance which is nearly the gold film resistance as shown in **Fig. 2**. The inner wall temperature of the tube T_{tube} can be calculated as the liner function of the resistance of the tube R_{tube}:

$$R_{tube} = a_{tube} T_{tube} + b_{tube} \tag{1}$$

, where a_{tube} and b_{tube} is the constant values, and these constant values can be determined by non-heating calibration test before boiling experiment.

In this study, the length of an electrode region which consists of an electrode and silver paste is 38 mm (19 mm on the inner wall and 19 mm on the outer wall of the tube), therefore the total length of two electrodes region at the both end of the tube is 76 mm. In contrast, the heated length of the tube, gold thin film region, is only 5 mm. So, the resistance of electrodes regions should be considerd for the estimation of the inner wall temperature. **Figure 4** shows the electro-structure of the tube and the measured temperature points. The outer wall temperature, T_{ow}, is mesured by k-type thermocouple, the fluid temperature, T_f, is calculate from the inlet and outlet temperatures of the test section. Here, assuming the temperatures of the gold film T_{gold}, electrode regions T_{elec} are liner functions of the each resistance, R_{gold} and R_{elec} :

$$R_{gold} = a_{gold} T_{gold} + b_{gold}, \tag{2a}$$

$$R_{elec} = a_{elec} T_{elec} + b_{elec} \tag{2b}$$

, where a_{gold}, a_{elec}, b_{gold}, b_{elec} are constant values, and T_{tube}, a_{tube}, b_{tube} in eq. (1) were already found from the results of non-heating calibration test as shown in **Fig. 3**.

In the case of non-heating calibration test, T_{tube}, T_{gold}, T_{elec} can be set the fluid temperature, T_f, under steady state condition. Thus, from the relation of $R_{tube} = R_{gold} + R_{elec}$,

$$a_{tube} T_f + b_{tube} = \left(a_{gold} + a_{elec}\right) T_f + \left(b_{gold} + b_{elec}\right). \tag{3}$$

So, the follwing relations are reduced:

$$a_{tube} = a_{gold} + a_{elec}, \quad b_{tube} = b_{gold} + b_{elec} \tag{4}$$

and

$$T_{tube} = \frac{a_{gold} T_{gold} + a_{elec} T_{elec}}{a_{tube}}. \tag{5}$$

The cross-section area of the silver paste of the electrode region, A, can be calculated from the measured weight of silver paste, therefore a_{elec} becomes

$$a_{elec} = \sigma_0 \frac{l}{A} \beta \tag{6}$$

, here l is the length of the electrode region, 76 mm, A is the cross-section area of the silver paste of the electrode region, 0.2415 mm^2, $\sigma_0 = 8.7 \times 10^{-7}$ Ω/ m and $\beta = 0.004\ K^{-1}$ are the electrical resistivity and the temperature coefficients of the silver paste, respectively.

Finally, assuming the temperature of the electrode region, T_{elec}, is an average temperature of T_{gold} and T_{ow}:

$$T_{elec} = \left(T_{gold} + T_{ow}\right)/2, \tag{7}$$

, T_{gold} can be derived from equations (4), (5), (6), (7).

In order to compare the measurements temperatures, T_{tube} and T_{gold}, with the correlations, Al-Arabi's correlation which is considered by the entrance effect is used for the predicted Nusselt number, Nu, for the turbulent single-phase flow[5] :

$$\frac{Nu}{Nu_\infty} = 1 + \frac{\frac{(z/D)^{0.1}}{Pr^{1/6}}\left(0.68 + \frac{3000}{Re^{0.81}}\right)}{z/D} \tag{8}$$

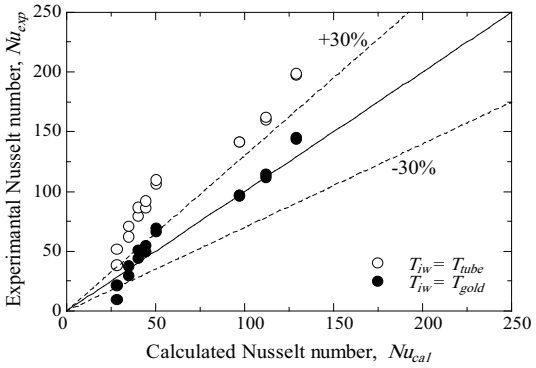

Fig. 5 Comparsion of Nusselt numbers calculated from eq. (10) for laminar flow and eq. (8) for turbulent flow (○: unconsidered electrode resistance; $T_{iw} = T_{tube}$, ●: considered electrode resistance; $T_{iw} = T_{gold}$).

, where z is the heated length of the tube, D is the inner diameter of the tube, Re is the Reynolds number, Pr is Prandtl number, Nu_∞ is the Nusselt number of a fully developed turbulent single-phase flow. Nu_∞ is calculated with Gnielinski's correlation[6]:

$$Nu_\infty = \frac{(f_w/8)\cdot(Re-1000)\cdot Pr}{1+12.7\,(f_w/8)^{1/2}\cdot\left(Pr^{2/3}-1\right)} \tag{9}$$

, where f_w is the wall friction coefficient, $f_w = 0.3164/Re^{1/4}$. For laminar flow heat transfer, Shah-London correlation[7] is applied for the fully developing flow;

$$Nu = 1.953\left(\frac{z}{D\cdot Re\cdot Pr}\right)^{-1/3}. \tag{10}$$

Figure 5 shows the experimental Nusselt numbers, Nu_{exp}, collected from the single-phase heat transfer experiment by using the short transparent heated tube, as compared with the Nusselt numbers Nu_{cal} calculated from eq. (10) for laminar flow and eq. (8) for turbulent flow. Here two temperatures, T_{tube} and T_{gold}, are considered as the inner wall temperature of the short tube to calculate Nu_{exp}. From the comparison of Nu_{exp} derived from two temperatures, Nu_{exp} which was used T_{gold} has a good agreement with Nu_{cal} than that of Nu_{exp} by using T_{tube}. Although two assumptions as equations (2) and (7) are still open questions, T_{gold} is applied for the inner wall temperature of the short transparent heated tube in this study.

2.3 Image Anaysis Procedure

One of the specialties of the transparent heated tube, flow behaviour can be observed through the tube wall. In this study image processing software ImageJ[8] was used to analyze the images obtained by high speed camera with 1000 fps. Various imformations such as film thickness of annular flow and passing of disturbance wave in rough can be obtained from the images.

Figure 6 shows an example of the image analysis procedure. Firstly, difference of brightness between liquid single-phase flow and gas-liquid two-phase flow is calculated for cancellation of the brightness distribution caused by curvature of the tube. Then, brightness difference image which can be used for brightness analysis is obtained. After that, the image is binarized to calculate liquid film thickness of annular flow. The pixcel size of the image anaylsis area, which is the same territory as the heated area, is about 104 pixels × 104 pixels, so the resolution of the film thickness calculation is approximately 50 μm by present image analysis method.

Figure 7 shows the transition of the brightness that is mean value of the entire area of the heated part under various heat flux, q_{in}, conditions. Mass velocity condition are almost same, $G = 35$ kg/m^2s, and the fluctuation of mass velocity in run is about ± 5 kg/m^2s. At the beginning of nucleate boiling, $q_{in} = 53.0$ kW/m^2, as shown in **Fig. 7(a)**, brightness value is almost constant and the time average brightness value is 157.8 that is the highest value among three heat flux conditions. For $q_{in} = 96.4$ kW/m^2, many bubbles comperaed with low heat flux case were found. The time

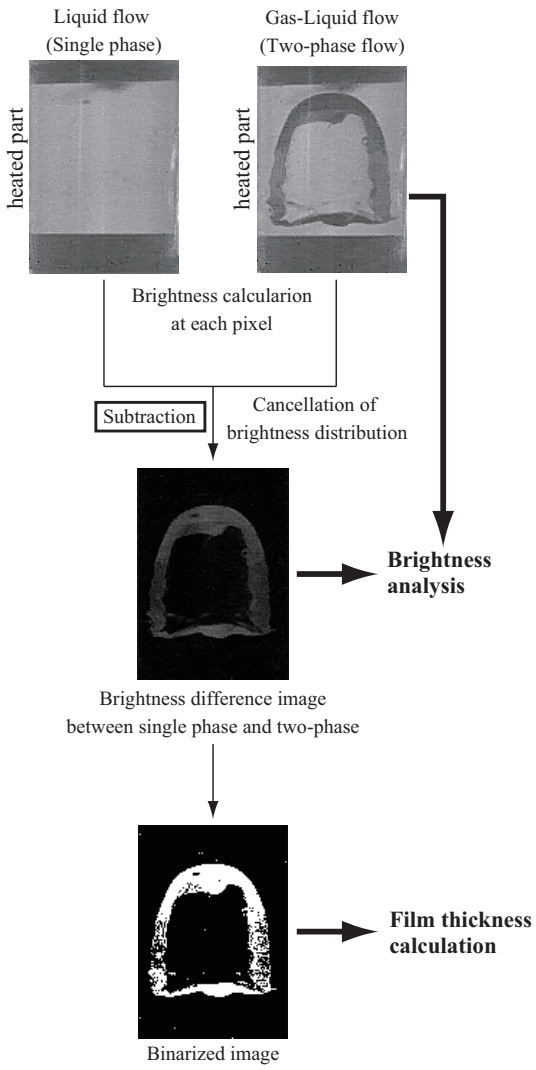

Fig. 6 Image analysis procedure.

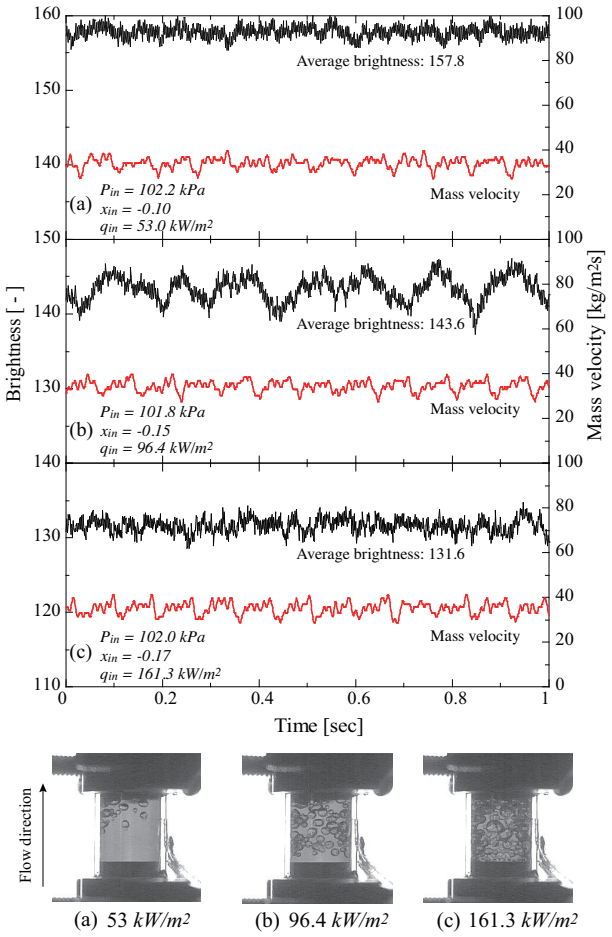

Fig. 7 An exapmple of the brightness analysis in the nucleate boiling region under different heat flux conditions. (a) $q_{in} = 53.0\ kW/m^2$, (b) $q_{in} = 96.4\ kW/m^2$, (c) $q_{in} = 161.3\ kW/m^2$.

average brightness value, 143.6, decreases with increasing heat flux, because the brightness at the gas-liquid interface of bubbles is lower than that of the liquid or gas single-phase region. Number of bubbles increases with increasing heat flux as shown in flow behaviour image in **Fig. 7**, so the time average brightness value decreases by the gas-liquid interface increment. In addition, the amplitude of brightness is larger than that of lower heat flux case, because it depends on cycle of bubble departure and generation from the heated wall. For the highest heat flux, q_{in} = 161.3 kW/m^2, the time average brightness value takes a minimun value, 131.6. In such a high heat flux condition, boiling bubble unintermitted generates with high bubble density, so the amplitude of brightness became small again same as lowest heat flux case.

3. Experimental results

Here, two experimental results, annular flow with disturbance wave and slug flow, are described. **Figure 8** shows the transition of mass velocity, brightness, inner wall temperature, heat transfer coefficient and flow behaviour under the condition of annular flow with disturbance wave. Note that brightness, inner wall temperature and heat transfer coefficient are the average value of the entire heated surface. The image data is obtained by high-speed camera with 1,000 fps and the temperature data and mass velocity are measured by data logger (DU1040-H, Takasago Ltd.) with 100 Hz. The time lag between them is less than ±0.02 s. The fluctuation of mass velocity is about $\pm 5\ kg/m^2s$ same as **Fig. 7**. The brightness value of annular flow is 160-165, and when passing of the disturbance wave, the brightness value declines drastically down to 140-150. For example, it was found that the distrabance wave was passing the tube at t = 0.508 s as shown in **Fig. 8(d)**. The transition of the inner wall temperature has same trend, the temperature decreases with the passing of the distrubance wave. The frequency of distarbance wave is about 10 Hz obviously from brightness data, and it is completly coincides with the inner wall temperature decrease. And the heat transfer coefficients, which are drived from heat flux, inner wall and fluid temperatures, increase slightly. Though the amplitude of inner wall temperature

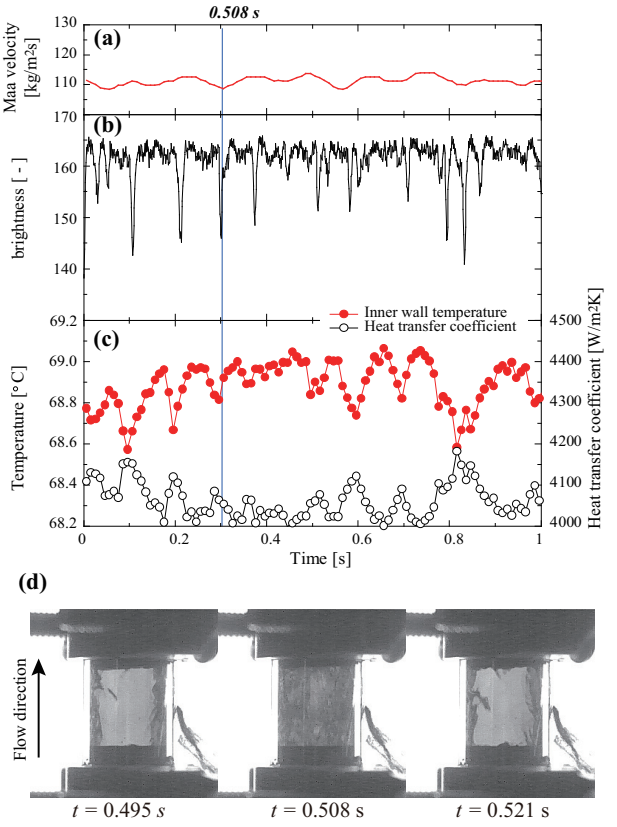

Fig. 8 The transition data of (a) mass velocity, (b) brightness, (c) inner wall temperature and heat transfer coefficient, and (d) images of flow behaviour under the conditions of annular flow with disturbance wave (q_{in} = 44.8 kW/m^2, G = 112.1 kg/m^2s, P_{in} = 96.4 kPa, x_{in} = 0.48).

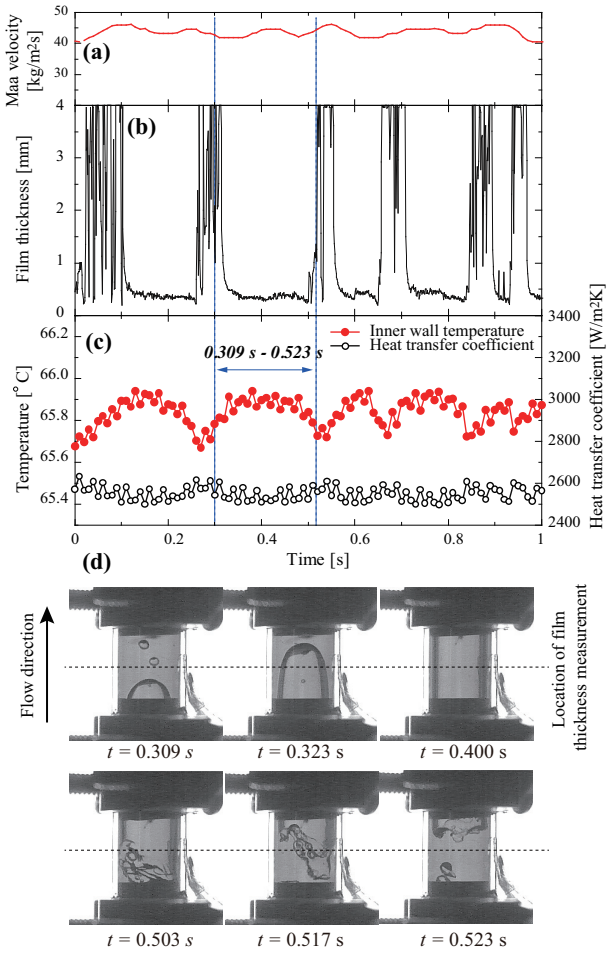

Fig. 9 The transition data of (a) mass velocity, (b) film thickness, (c) inner wall temperature and heat transfer coefficient, and (d) images of flow behaviour under the conditions of slug flow ($q_{in} = 22.0\ kW/m^2$, $G = 44.0\ kg/m^2s$, $P_{in} = 98.3$ kPa, $x_{in} = 0.11$).

is very small, 0.2-0.5 K, the transparent heated short tube can be detected this temperature variation crearly.

The transition data under slug flow conditions is shown in **Fig. 9**. The liquid film thickness which drived from a brightness data was measured at the center line of the heated length. Though the film thickness data is rough value by this anaylsis method, this data is very useful because presence of slug can be decided objectively. When a slug is passing through the tube, the film thickness can be detected. For example, the slug was passing the tube from $t = 0.309$ s to $t = 0.523$ s as shown in **Fig. 9(d)**. The film thickness declined drastically less than 1 mm, and the thickness value was taken almost constant, approximately 0.5 mm, during this period. After passing of the slug, the film thickness was rised again. The inner wall temperature was increased when the slug came into the center line of the tube, then the temperature was obtain the constant value during the existance of the liquid film of the slug. The temperature was decreased slightly when the rear of the slug was reached at the center line of the tube. This temperature decrease was caused by turbulent flow at the wake of slug. The heat transfer coefficient was changed corresponding inner wall temperature fluctuation.

Three zone model which was proposed by J. Thome et al.[9] was indicated that the heat transfer in the thin liquid film evaporation region is typically on the order of several times that of the liquid flow region. This three zone model is applied for heat transfer in microtube. In contrast, present study is used a tube which has 4 mm of the inner diameter. This tube diameter is not microtube for the present test fluid, FC-72, so the liquid film of this study is thicker than that of three zone model case. Heat resistance of the liquid film increases in proportion to liquid film thickness. So the heat transfer deterioration is occurred at the liquid film region of slug.

4. Conclusions

The transparent heated short tube, which is installed in the third segment of the glass heated section of the flow boiling and two-phase flow experimental facility on boad the International Space Station. In this study, derivation of the inner wall temperature and image analysis of flow behavior by using the short tube was described. Then the relation between heat transfer characteristics and flow behavior was discussed. the conclusions are as follows;

1. To estimate the inner wall temperature of the short tube, the gold thin film resistance, R_{gold}, is applied instead of total resistance of the tube, R_{tube}. As a result of single-phase heat transfer experiment, Nusselt number drived from R_{gold} has a good agreement with existing correlations compared to Nusselt number by using R_{tube}.

2. Performing the analysis of flow behaviour image, liquid film thickness of annular flow and passing of disturbance wave in rough can be obtained with heat transfer characteristics data simultaneously.

3. In the conditions of this study, the heat transfer of the liquid film in slug flow is insignificantly small compeared to turbulent liquid flow at the wake of slug.

Acknowledgments

The authors express appreciation for the support of TPF project by JAMSS, JSF, IA and for the useful discussions with International Topical Team of boiling and two-phase flow.

References

1) K. Fujii, M. Komasaki, T. Kurimoto, H. Kawasaki, K. Sawada, K. Suzuki, H. Asano, O. Kawanami, R. Imai, Y. Shinmoto and H. Ohta: J. Phys. Sci. Appl., **2** (2012) 71.
2) H. Ohta: Nuclear Engineering and Design, **175** (1997) 167.
3) H. Ohta: Advances in Heat Transfer, **37** (2003) 1.

4) O. Kawanami, H. Azuma and H. Ohta: Int. J. Heat Mass Trans., **50** (2007) 3490.
5) M. Al-Arabi: Heat Trans. Eng., **3** (1982) 76.
6) V. Gnielinski: Int. Chem. Eng., **16** (1976) 359.
7) R. Shah and A. London: Academic Press, New York, (1978) 128.
8) C. Schneider, W. Rasband and K. Eliceiri: Nature Methods, **9** (2012) 671.
9) J. Thome, V. Dupont and A. Jacobi: Int. J. Heat Mass Transfer, **47** (2004) 3375.